Electrochemical behavior of cocaine cutting agents at the polarized liquid-liquid interface

Borgul, Paulina; Sobczak, Karolina; Rudnicki, Konrad; Glazer, Piotr; Pawlak, Patrycja; Trynda, Anna; Skrzypek, Sławomira; Poltorak, Lukasz

DOI
10.1016/j.electacta.2021.139553

Publication date
2022

Document Version
Final published version

Published in
Electrochimica Acta

Electrochimica Acta 402 (2022) 139553

Contents lists available at ScienceDirect

Electrochimica Acta

journal homepage: www.elsevier.com/locate/electacta

Electrochemical behavior of cocaine cutting agents at the polarized liquid-liquid interface

Paulina Borgul[a], Karolina Sobczak[a], Konrad Rudnicki[a], Piotr Glazer[b], Patrycja Pawlak[a], Anna Trynda[c], Sławomira Skrzypek[a], Lukasz Poltorak[a,*]

[a] Department of Inorganic and Analytical Chemistry, Electroanalysis and Electrochemistry Group, Faculty of Chemistry, University of Lodz, Tamka 12, 91-403 Lodz, Poland
[b] Chemical Engineering, Delft University of Technology, the Netherlands
[c] Chemistry Department, Central Forensic Laboratory of the Police, Warsaw, Poland

ARTICLE INFO

Article history:
Received 6 September 2021
Revised 4 November 2021
Accepted 4 November 2021
Available online 9 November 2021

Keywords:
Illicit drugs
ITIES
Ion partition diagrams
Cocaine sensor
Adulterants
Voltammetry

ABSTRACT

In this work, we have used cyclic voltammetry to investigate the interfacial behavior of cocaine cutting agents at the electrified liquid-liquid interface formed between a solution of the water and 1,2-dichloroethane phases. Among 27 chemical species used to adulterate cocaine street samples, only 8 were detectable in the available potential window. These include procaine, lidocaine, levamisole, hydroxyzine, caffeine, phenylethylamine, diltiazem, and diphenhydramine. From the calibration curves obtained using voltammetric data, we have extracted the electroanalytical parameters such as detection sensitivities, limits of detection, and limits of quantifications. Also, for each electrochemically active drug, we have calculated diffusion coefficients and plotted the ion partition and concentration fraction diagrams. All this information is discussed in a view of the cocaine sensors development focused on its detection from demanding matrix defined by the street samples composition.

1. Introduction

The estimate from 2009 states that 210 million people used illicit drugs, which equals around 4.8% of the world's population. The report states that in 2018 this number grew to 269 million and 5.3%, respectively. This problem increases much faster in developed as compared with developing countries. Adolescents and young adults make the largest group of recreational drug users [1]. These trends are directly responsible for the additional economic load on our society. Another worrying issue is the rapid development of new drugs (known as NPS - new psychoactive substances). In 2018, there were 541 different NPS on the black market, 48 of which were previously unknown [1]. Scientists around the world are constantly taking steps to counteract drug addiction. Control, quick and simple sample analysis is extremely important in this respect.

Many analytical techniques are routinely used to detect narcotic substances. These include Gas Chromatography with Flame Ionization Detection (GC/FID) [2], Gas Chromatography- Tandem Mass Spectrometry (GC/MS/MS) [3], High-Performance Liquid Chromatography (HPLC) [4], Liquid Chromatography with Tandem Mass Spectrometry (LC/MS /MS) [5], Fourier Transformed Infrared Spectroscopy (FTIR) [6], Raman spectroscopy [7], or even Scanning Electron Microscopy-Energy Dispersive X-ray Spectroscopy (SEM/EDX) [8]. In the last few years, the electroanalysis of illicit drugs has also attracted a lot of attention. Electrochemical sensors cannot compete with spectroscopy and spectrometry-based techniques as the latter provide significantly higher selectivity. However, due to compactness, low cost, and still highly reliable output, some electroanalytical solutions may fulfill the requirements of the presumptive illicit drugs detection [9–12]. The electroanalytical investigation of street samples is complicated by the co-existence of the targeted drug with substances generally known as cutting agents. These chemical species may interfere with the detection of narcotic substances and thus distort the analysis result [13]. Cutting agents are added to the street samples due to a few reasons, such as (i) increasing the profit of drug retailers as the overall drug content is reduced, (ii) cutting agents may affect the pharmacological effect of the drug and finally (iii) the analytical screening of some mixtures can be problematic, and hence, it may lead to complicated detection protocols [14]. The chemical substances frequently used

* Corresponding author.
E-mail address: lukasz.poltorak@chemia.uni.lodz.pl (L. Poltorak).

https://doi.org/10.1016/j.electacta.2021.139553

as cutting agents include talc, milk powder, starch, sugars, but also active analgesics, stimulants, nootropic or antiallergic agents [15]. According to the European Drug Report, the average purity of cocaine retailed on the black market in Europe in 2018 ranged from 23% to 87%. In the first six months of 2019, cocaine was the most frequently distributed substance in Europe according to the European Monitoring center for Drugs and Drug Addiction. 1011 cocaine samples subjected to analytical screening revealed that 57% of the samples contained only the drug and inactive compounds, while 40% were found to be in combination with one or more pharmacologically active cutting agents. The most commonly added adulterants were levamisole (18,2%), caffeine (14,4%), phenacetin (9,7%) and lidocaine (4,2%) [16]. Cocaine street samples, seized in Poland in 2018–2019, were very pure and contained between 64 and 99% of cocaine. The most commonly used adulterants were levamisol, caffeine, benzocaine, lidocaine and procaine [17].

The result of the illicit drugs screening protocols used in forensic analytical laboratories, usually chromatographic techniques coupled to mass spectrometry, sometimes may lead to false negatives or false positives in the presence of cutting agents existing in street samples [18]. Also, for electrochemical methods the challenge is to develop a selective sensing interface. It is often desirable to modify the electrodes to adjust selectivity and improve detection limits. Florea *et al*. used a graphene-modified screen printed electrodes functionalized by the electrodeposition of two polymers (starting from o-phenylenediamine or p-aminobenzoic acid monomers) for the analysis of cocaine in the presence of levamisole [19]. The utilization of the latter monomer allowed for the construction of a sensor providing better electroanalytical parameters, and hence, it was selected as the optimal one. Good selectivity for MDMA (3,4-methylenedioxymethamphetamine) and morphine was achieved using a sensor modified with high surface area carbon nanohorns decorated with Pt nanoparticles (CNHs@PtNPs). It allowed the detection of both substances starting from very low concentrations of circa 20 nM [20]. Parrilla et al., developed a method for the determination of amphetamine (requiring earlier derivatization) at graphite screen-printed electrodes (SPEs). The effect of the common cutting agents on the signal originating from functionalized amphetamine was also tested to evaluate sensor selectivity [21]. Since the majority of illicit drugs are amines, the electroanalytical protocols developed for their direct analysis are usually based on carbon electrodes (bare or modified with nanomaterials like e.g. carbon nanotubes, graphene oxide). Amine oxidation over carbon-based support may lead to the formation of a stable covalent linkage between carbon surface and the nitrogen atom, and hence, electrode passivation [22,23]. Another issue related to illicit drugs sensing from the street sample at carbon and other types of solid electrodes is the nature of the cutting agents that frequently contain amine functionalities undergoing oxidation at similar potential values as the target analytes [13,24]. These two drawbacks can be partly overcome by replacing carbon-based electrodes with the interface between two immiscible electrolyte solutions (ITIES) as this can be easily renewed (solution to fouling and passivation) and allows for the detection not limited to redox reactions (sensing at ITIES mainly result from interfacial ion transfer). The most commonly used ITIES experimental configuration consists of an aqueous solution of a highly hydrophilic salt contacted to an organic solvent being a solution of a strongly hydrophobic salt [25]. The soft junction formed between these two solutions can be polarized and further used to study interfacial charge transfer of i.e., ion, electron, facilitated ion transfer, or conjugated ion and electron transfer reactions [26]. These interfacial reactions can find applications in broadly defined analytical chemistry [27,28]. ITIES can be applied in ion extraction [29], electrochemical sensing [30], or biomimetic junctions formation [31]. Existing reports cover a wide range of target analytes including drugs [32,33], biomolecules [34,35] such as amino acid [36,37], and proteins [38]. ITIES can be also employed as the sensors for illicit drugs (e.g. cocaine) detection [39]. A number of pharmaceuticals classified as psychoactive substances, including cocaine cutting agents, holding amine group within their structure were also investigated at the electrified LLI: lidocaine, dicaine [40], hydroxyzine [41], procaine [42], dopamine [43], γ-aminobutyric acid [44], and a number of opioids and amphetamine-type drugs. [45] The superior properties of the ITIES based sensing platform for illicit drugs detection requires comprehensive study devoted to the determination of the interfacial properties of the cutting agents frequently found in street samples.

In this work, we have comprehensively studied 23 cocaine cutting agents at the polarized liquid-liquid interface (LLI) formed between aqueous sodium chloride solution or Britton Robinson buffer (BRB), and bis(triphenylphosphoranylidene)ammonium tetrakis(4-chlorophenyl)borate (BTPPATPBCl) dissolved in 1,2-dichloroethane. Tested chemical species included sugars, inorganic salts, inorganic acids, and organic compounds. With cyclic voltammetry we have defined and calculated a number of electrochemical, electroanalytical, and physicochemical parameters such as limits of detection (LODs), limits of quantification (LOQs), voltammetric detection sensitivity, diffusion coefficients, standard Galvani potentials of the ion transfer reaction ($\Delta^{aq}_{org}\Phi\odot$), standard Gibbs free energy of the ion transfer reaction ($\Delta^{aq}_{org}G\odot$), water – 1,2-dichloroethane partition coefficients ($\log P\odot_{aq/org}$) and finally defined the experimental conditions governing the cutting agents interfacial activity/inactivity. These results build guidelines for the development of the illicit drugs street samples sensors that are based on ITIES.

2. Methods and materials

2.1. Materials

D-Glucose anhydrous (Fisher chemical, M = 180.16 g•mol^{-1}), D-Maltose monohydrate (≥ 99%, Sigma-Aldrich, M = 360.31 g•mol^{-1}), D-(-)-Fructose (≥ 99%, Sigma-Aldrich, 180.16 g•mol^{-1}), α-Lactose monohydrate (Sigma-Aldrich, M = 360.31 g•mol^{-1}), D-(+)-Saccharose (≥ 99%, Acros Organics, M = 342.29 g•mol^{-1}), D-(-)-Mannitol (≥ 99%, Fisher Chemical, M = 182.17 g•mol^{-1}), sodium carbonate anhydrous (Na_2CO_3, ChemPur, M = 105.99 g•mol^{-1}), sodium bicarbonate ($NaHCO_3$, pure, ChemPur, M = 84.01 g•mol^{-1}), boric acid (H_3BO_3, pure, ChemPur, M = 61.83 g•mol^{-1}), acetylsalicylic acid (99%, Sigma, M = 180.16 g•mol^{-1}) creatine hydrochloride (≥ 97%, Sigma, M = 149.58 g•mol^{-1}), 2-phenylethylamine (99%, Acros Organics, M = 121.18 g•mol^{-1}), diphenhydramine (≥ 98%, Sigma-Aldrich, M = 108.14 g•mol^{-1}), phenacetin (≥ 98%, Sigma, M = 179.22 g•mol^{-1}) griseofulvin (97%, Acros Organics, M = 352.76 g•mol^{-1}), levamisole hydrochloride (Chemat, M = 240.75 g•mol^{-1}), hydroxyzine dihydrochloride (Chemat, M = 447.83 g•mol^{-1}), diltiazem (Sigma-Aldrich, M = 450.98 g•mol^{-1}), paracetamol (Synoptis Pharma, tablets, paracetamol concentration 0.89 g/g, M = 151.16 g•mol^{-1}), caffeine (98.5%, Argenta, M = 194.19 g•mol^{-1}), benzocaine (≥ 99%, Sigma-Aldrich, M = 165.19 g•mol^{-1}), procaine hydrochloride (≥ 97%, Sigma, M = 272.77 g•mol^{-1}), lidocaine (97.5%, Acros Organics, M = 234.34 g•mol^{-1}) were all used as received. Sodium chloride (NaCl, ChemPur M = 58.44 g•mol^{-1}), phosphoric acid (H_3PO_4, 80%, ChemPur, M = 97.99 g•mol^{-1}), acetic acid (CH_3COOH, > 99.5%, ChemPur, M = 60.05 g•mol^{-1}) and boric acid (H_3BO_3, pure, ChemPur, M = 61.83 g•mol^{-1}) were used to prepare Britton-Robinson buffer (BRB).

The aqueous phase used to form ITIES was either 10 mM NaCl solution or 10 mM NaCl in a BRB buffer with a pH in the range from 2 to 11. The value of pH was adjusted with 1 M NaOH. BRB buffer was prepared from a stock solution of the buffer matrix con-

taining 0.04 M of a mixture of boric acid (H_3BO_3), ortho phosphoric acid (H_3PO_4), and acetic acid (CH_3COOH). The desired pH value for BRB was adjusted with a pH meter (Orion STAR, A111, The Netherlands) using a polymer pH electrode (Polilyte Lab, Hamilton, Switzerland).

Bis(triphenylphosphoranylidene) ammonium tetrakis(4-chlorophenyl)borate was obtained by reacting a potassium tetrakis(4-chlorophenyl)borate (KTPBCl, ≥ 98%, Sigma-Aldrich) with bis(triphenylphosphoranylidene)ammonium chloride (BTPPACl, 97%, Sigma-Aldrich) [46]. 1,2-dichloroethane (1,2-DCE) was used as the solvent for the organic phase.

2.2. Electrochemical cell

All experiments described in this work were conducted in a classical macroscopic electrochemical glass cell dedicated to the LLI-based experiments (see ESI Fig. S1). Four electrodes were used to polarize the ITIES. The aqueous phase counter electrode (Pt wire) was always placed in the main/middle compartment of the cell. The organic phase counter electrode (Pt wire sealed in glass capillary) was crossing the upper aqueous phase and was situated at the cell bottom in the organic phase. Silver/silver chloride wires (Ag/AgCl) served as the reference electrodes. The aqueous phase reference electrode was directly contacted with the aqueous phase through the upper Luggin capillary. The organic phase reference electrode was placed in the aqueous phase solution (containing common cation with the organic phase background electrolyte) being contacted with the organic phase in the bottom Luggin capillary. Electrochemical measurements were performed using an Autolab 302N from Methrom (Metrohm Autolab B.V., The Netherlands) operated via NOVA 1.11.

Cell I shows the composition of the electrochemical system used in this study:

$$Ag|AgCl|\begin{matrix}10\ mM\ NaCl\ 10\ mM\ HCl\ and/or\ BRB\\ x\ \mu M\ cutting\ agent\end{matrix}||\begin{matrix}5\ mM\\ BTPPATPBCl\end{matrix}|\begin{matrix}10\ mM\ NaCl\\ 10\ mM\ BTPPACl\end{matrix}|AgCl|Ag \quad \text{(Cell I)}$$

By definition, the interfacial potential difference is defined as the potential of the aqueous phase minus the potential of the organic phase. The sign of the recorded currents is attributed to the following interfacial ion transfer reactions: positive currents – cation transfer from the aqueous to the organic phase or anion transfer from the organic to the aqueous phase; negative currents – cation transfer from the organic to the aqueous phase or anion transfer from the aqueous to the organic phase.

2.3. Data treatment

Unless otherwise stated, values of the peak currents in all measurements were determined by subtracting the capacitive current from the current values defined by peak height. Since caffeine ion transfer was overlaid with the transfer of ions limiting the potential window, the current values plotted on the corresponding calibration curve were obtained after blank (voltammogram recorded before the analyte addition) reading subtraction.

The formal ion transfer potential for all studied interfacially active cocaine cutting agents was calculated using the internal standard method. The Galvani potential scale of cyclicvoltammograms subject to calculations was corrected using tetramethylammonium cation formal Galvani ion transfer potential ($\Delta^{aq}_{org}\phi'_{TMA^+} = 160$ mV) [47]. The formal Galvani potential of the studied cocaine cutting agents was calculated using the following relationship:

$$\Delta^{aq}_{org}\phi'_{TMA^+}\,\Delta^{aq}_{org}\phi'_{Drug^+} = \Delta^{aq}_{org}\phi^{"+"peak}_{TMA^+}\,\Delta^{aq}_{org}\phi^{"+"peak}_{Drug^+} \quad (1)$$

where $\Delta^{aq}_{org}\phi'_{Drug^+}$ is the formal Galvani ion transfer potential for the studied cocaine cutting agent, $\Delta^{aq}_{org}\phi^{"+"peak}_{TMA^+}$ is the forward (positive) peak position of TMA^+ on non-calibrated potential difference scale and $\Delta^{aq}_{org}\phi^{"+"peak}_{Drug^+}$ is the forward (positive) peak position of cocaine cutting agent on non-calibrated potential difference scale.

3. Results and discussions

In Table 1 we have summarized all cocaine cutting agents (chosen based on literature overview and the knowledge originating from the Central Forensic Laboratory of the Police, Poland) [17,48,49] subjected to comprehensive analysis at the electrified LLI. In first, we have performed the logical evaluation of the interfacial activity of tested compounds to simply list the molecules that may undergo electrochemically controlled simple interfacial ion transfer reaction giving a signal within the available potential window. At this point, it is relevant to mention that the limiting currents on the lower and higher potential scale are originating from the interfacial transfer of the background electrolyte ions. On the less positive side of the potential window the limiting currents will be originating from the interfacial transfer of the aqueous phase background electrolyte anions (chloride, phosphate, borate, or/and acetate), since the standard Galvani potential of the most hydrophilic anion transfer (chloride, $\Delta\phi_{1/2} = -0.53$ V) is significantly different from the standard Galvani potential of the $BTPPA^+$ transfer ($\Delta\phi_{1/2} = -0.70$ V). Aqueous phase cations (H^+ or Na^+) are expected to limit the potential window on the more positive side. Also, at pH > 5, the potential window limiting currents originating from the transfer of Na^+ from the aqueous to the organic phase may overlay with $TPBCl^-$ transfer from the organic to the aqueous phase. For tested sugars (glucose, maltose, fructose, lactose, saccharose, and mannitol – see ESI Fig. S2-S7) no additional signals within the available potential window have been recorded. The pKa values for saccharides are rather high (>12) [50], and hence, in the entire studied pH range investigated molecules will be neutral and as expected will not experience the potential difference drop across the ITIES. Dissociation and generation of a negative charge within sugars structure may happen at pH close to or higher than 12. Such conditions are not interesting from the amine-based illicit drugs sensing perspective since these will be deprotonated and hence interfacially inactive.

Inorganic chemical species such as sodium carbonate, sodium bicarbonate, and boric acid (see ESI Figs. S8–S10) have the ability to dissociate into ions when dissolved in the aqueous phase. The interfacial transfer of the resulting charged cationic or anionic species across the polarized LLI most probably overlays with or happens beyond Galvani potential difference defining the transfer of the background electrolyte ions. As such, these cutting agents should not directly affect the interfacial properties of the cocaine and other amine-based illicit drugs which may transfer within the available potential window. The indirect influence of the mentioned cutting agents is related to the fact, that these inorganic salts can buffer, and hence, affect the pH of the aqueous phase. Since the concentration fraction and interfacial properties of amine-based illicit drugs are pH-dependent, the experimental design of the envisaged sensor should ensure the fixed proton concentration being insensible to the analyte together with its matrix addition. The remaining class of cutting agents is defined as organic compounds known as pharmaceuticals or biologically active substances. Acetylsalicylic acid has a carboxyl group in its structure (pKa value 3.49 [51]), which under appropriate pH conditions may partially dissociate into carboxylate anion and proton (up to a value of about 3.5). However, neither the proton (its transfer overlays with the transfer of sodium cations) nor the obtained anion gave a signal in the potential window (see ESI Fig. S11). Below this pH value, the compound is in a neutral form in solution. Griseofulvin (see ESI Fig. S12) has ketone and ester groups within its structure which under studied experimental conditions remain neutral,

Table 1
Cocaine cutting agents studied at ITIES. Chemical structures and indications about interfacial activity/inactivity of the studied chemical species are given.

Name	Structure	Activity	Name	Structure	Activity	Name	Structure	Activity
1. Glucose	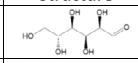	**Inactive**	9. Boric Acid	H_3BO_3	**Inactive**	17. Levamisole	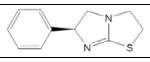	**Active**
2. Maltose	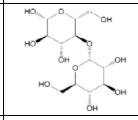	**Inactive**	10. Acetylsalicylic Acid	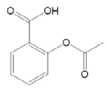	**Inactive**	18. Diltiazem	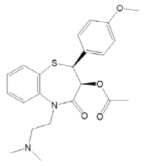	**Active**
3. Fructose	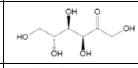	**Inactive**	11. Creatine	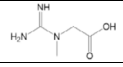	**Inactive**			
4. Lactose	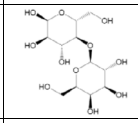	**Inactive**	12. 2-Phenylethylamine	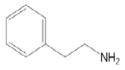	**Active**	19. Paracetamol	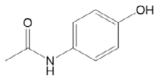	**Inactive**
5. Saccharose	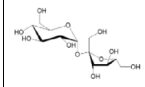	**Inactive**	13. Diphenhydramine	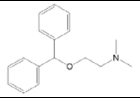	**Active**	20. Caffeine	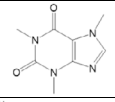	**Active**
6. Mannitol	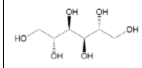	**Inactive**	14. Phenacetin	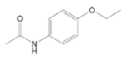	**Inactive**	21. Benzocaine	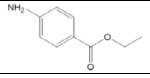	**Inactive**
7. Sodium Carbonate	Na_2CO_3	**Inactive**	15. Griseofulvin	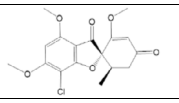	**Inactive**	22. Procaine	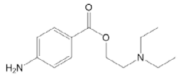	**Active**
8. Sodium Bicarbonate	$NaHCO_3$	**Inactive**	16. Hydroxyzine	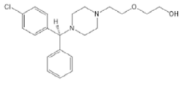	**Active**	23. Lidocaine	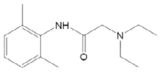	**Active**

and hence, ensure this compound inactivity at ITIES. We have obtained the same results for phenacetin and paracetamol (see ESI Figs. S13 and S14) holding an amide group. Additionally, chemical constituents of the tablet (fillers) this is polyvinylpyrrolidone, corn starch, sodium carboxymethylstarch, and stearic acid did not give a signal for the given experimental conditions. With two amine groups, which can easily be protonated giving the overall positive charge, we did not record the signal for creatine in the studied pH range (2–11) (see ESI Fig S15). Benzocaine is an example of a pharmaceutical that, despite the presence of an amine functionality, did not give a clear signal at the ITIES (see ESI Fig. S16). At studied concentration, benzocaine ion transfer is entirely overlaid with the H^+ transfer from the aqueous to the organic phase (positive current) and can be only observed after blank reading subtraction [39]. The lowest employed pH value being equal to 2 did not suffice to reach a high concentration fraction of protonated (positively charged) benzocaine molecule having relatively low pKa (~2.5) [52]. 2-phenylethylamine, diphenhydramine, hydroxyzine, levamisole, diltiazem, caffeine, procaine, and lidocaine were also investigated and were found to give a clear signal within the available potential window. For these compounds, clear signals were obtained at polarized LLI. These chemical species were subjected to comprehensive studies.

Compounds marked in Table 1 as active at the polarized LLI were subjected to an electroanalytical assessment. Each of the eight interfacially active compounds was initially dissolved in the aqueous phase, which was a solution of 10 mM NaCl and 10 mM HCl (pH 2). At given protons concentration, all cutting agents were fully charged (pH << pKa) meaning that the recorded signals follow the simple interfacial ion transfer reaction. Fig. 1 shows the cyclic voltammograms (ITVs) recorded for the increasing concentration of all chosen compounds. To transfer the protonated molecules (cations) from the aqueous to the organic phase, the LLI was polarized towards more positive potentials on the forward scan giving a positive peak current. The reversed scan was always stating at the positive end of the cyclic voltammogram and was going towards negative potential values. The peak current signals recorded during this process were due to the cation back transfer from the organic to the aqueous phase. The transfer of all studied species was reversible as indicated by the shape of the curves and the forward and reversed peak current ratio being found around unity. For procaine (Fig. 1-A), lidocaine (Fig. 1-B), levamisole (Fig. 1-C), hydroxyzine (Fig. 1-D), phenylethylamine (Fig. 1-F), diltiazem (Fig. 1-G), diphenhydramine (Fig. 1-H) the analyzed concentration range was from 3 µM to 100 µM. Since the ionic currents attributed to the caffeine (Fig. 1-E) ion transfer were strongly overlaid with the limiting currents values originating from the sodium and proton interfacial transfer, its quantification at lower concentrations was impossible. Thence, the calibration of caffeine took place in the range from 100 to 500 µM. Based on the obtained results we have plotted the calibration curves that can be found in Fig. 1 on the right from the corresponding cyclic voltammograms.

Using the linear fit equations from the positive and negative current values we have calculated a number of electroanalytical parameters which are summarized in Table 2. The lower limit of detection (LOD) for each compound is calculated using the following equation:

$$LOD = \frac{3.3 \cdot SD}{S} \quad (2)$$

whereas and the limit of quantification (LOQ) was obtained by proper substitution to eq. 3:

$$LOQ = \frac{10 \cdot SD}{S} \quad (3)$$

where SD and S are the standard deviation of the intercept and the slope of the calibration curve, respectively (values taken from the parameters of the linear fit equation). The sensitivity of the voltammetric detection is defined as the slope of the calibration

Table. 2
The summary of the electroanalytical and physicochemical parameters calculated or taken from the literature for the interfacially active cocaine cutting agents.

Name	Procaine	Caffeine	Lidocaine	Levamisole	Hydroxyzine	Phenethylamine	Diltiazem	Diphenhydramine
z	1	1	1	1	2	1	1	1
pK_a	8.9[55]	10.4[56]	7.9[57]	9.5[58]	2.1 and 7.1[59]	9.8[60]	7.5[61]	9.0[62]
LOD (+) / M	$5.12 \bullet 10^{-6}$	$1.57 \bullet 10^{-4}$	$8.37 \bullet 10^{-6}$	$9{,}73 \bullet 10^{-6}$	$2.45 \bullet 10^{-5}$	$3.20 \bullet 10^{-6}$	$1.00 \bullet 10^{-5}$	$2.57 \bullet 10^{-6}$
LOD (-) / M	$7.24 \bullet 10^{-6}$	$1.32 \bullet 10^{-4}$	$6.79 \bullet 10^{-6}$	$8.76 \bullet 10^{-6}$	$2.99 \bullet 10^{-5}$	$4.58 \bullet 10^{-6}$	$1.83 \bullet 10^{-5}$	$5.75 \bullet 10^{-6}$
LOQ (+) / M	$1.54 \bullet 10^{-5}$	$4.70 \bullet 10^{-4}$	$2.51 \bullet 10^{-5}$	$2.92 \bullet 10^{-5}$	$7.34 \bullet 10^{-5}$	$9.60 \bullet 10^{-6}$	$3.01 \bullet 10^{-5}$	$7.70 \bullet 10^{-6}$
LOQ (-) / M	$2.17 \bullet 10^{-5}$	$3.95 \bullet 10^{-4}$	$2.04 \bullet 10^{-5}$	$2.63 \bullet 10^{-5}$	$8.98 \bullet 10^{-5}$	$1.37 \bullet 10^{-5}$	$5.49 \bullet 10^{-5}$	$1.72 \bullet 10^{-5}$
Sensitivity (+) / $A \bullet M^{-1}$	0.187 ± 0.005	0.071 ± 0.010	0.147 ± 0.007	0.199 ± 0.010	0.118 ± 0.010	0.160 ± 0.002	0.161 ± 0.006	0.172 ± 0.003
Sensitivity (-) / $A \bullet M^{-1}$	0.128 ± 0.005	0.061 ± 0.007	0.132 ± 0.005	0.203 ± 0.009	0.105 ± 0.011	0.132 ± 0.003	0.184 ± 0.014	0.168 ± 0.006
D (+) / $cm^2 \bullet s^{-1}$	$4.78 \bullet 10^{-6} \pm 1.01 \bullet 10^{-6}$	$1.52 \bullet 10^{-6} \pm 5.55 \bullet 10^{-7}$	$3.25 \bullet 10^{-6} \pm 6.20 \bullet 10^{-7}$	$4.32 \bullet 10^{-6} \pm 7.55 \bullet 10^{-7}$	$1.32 \bullet 10^{-6} \pm 5.58 \bullet 10^{-7}$	$7.38 \bullet 10^{-6} \pm 3.19 \bullet 10^{-7}$	$1.11 \bullet 10^{-5} \pm 1.13 \bullet 10^{-5}$	$2.27 \bullet 10^{-6} \pm 7.55 \bullet 10^{-7}$
$\Delta^{aq}_{org}\Phi \odot$ /V	0.110	0.272	0.005	−0.049	−0.019	0.271	−0.094	−0.091
$\Delta^{aq}_{org}G'$ / J•mol^{-1}	−10,622.99	−26,272.87	−458.30	4698.82	3608.54	−26,137.79	9069.59	8731.89
$\log P'_{aq/org}$	−1.93	−4.76	−0.08	0.85	0.65	−4.74	1.64	1.58
K_D	6.5	–	520	1500	130	0.1	190	15,000
$pH_{[Drug^+_{aq}]=[Drug_{org}]}$	8.0	–	5.2	6.3	4.9	9.7	5.3	4.8

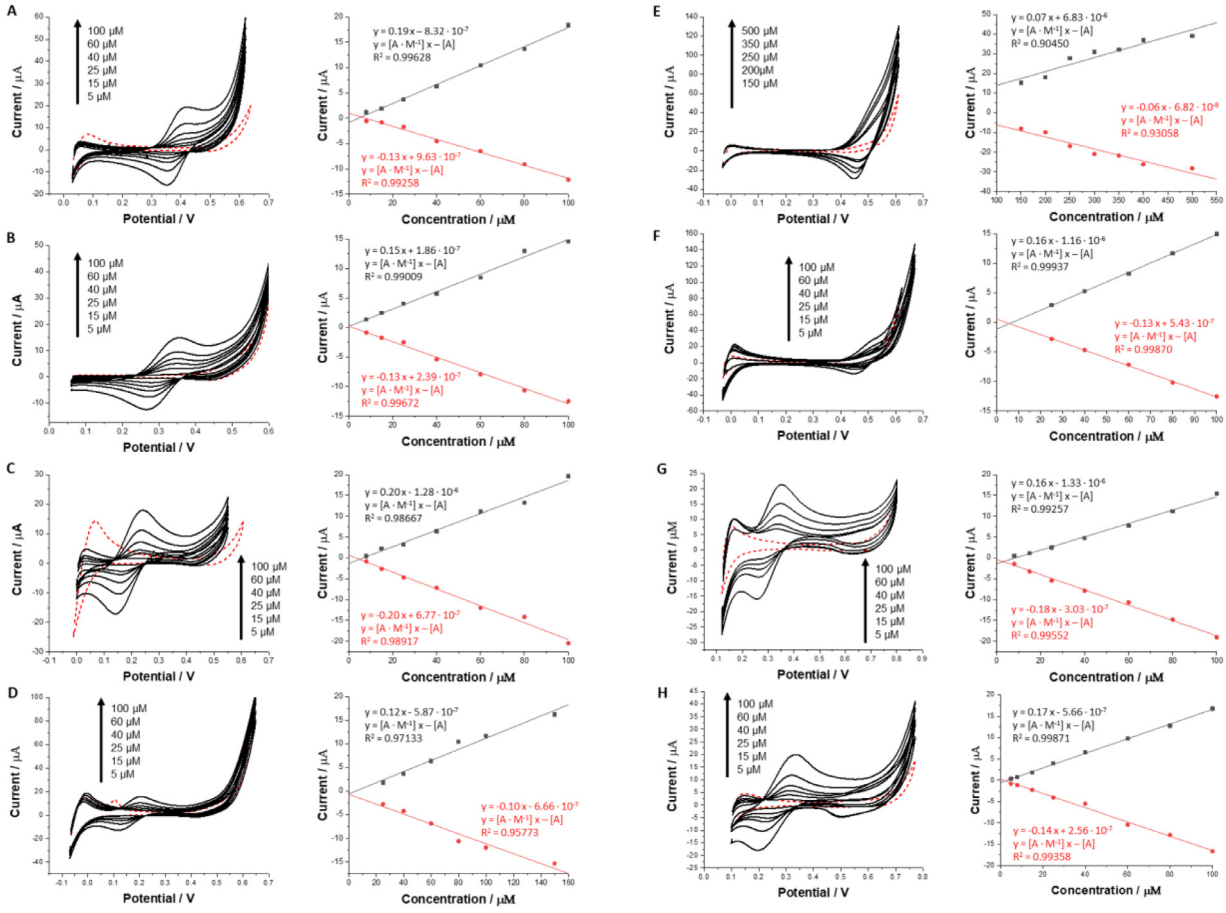

Fig. 1. Cyclic voltammograms were recorded for the increasing concentration of studied cocaine cutting agents (A - procaine, B - lidocaine, C - levamisole, D - hydroxyzine, E - caffeine, F - phenethylamine, G - diltiazem, H - diphenhydramine) with corresponding positive and negative peak current intensities plotted in a function of a drug concentration. The scan rate was 25 mV•s^{-1}. pH was equal to 2 (aqueous phase was 10 mM NaCl, 10 mM HCl). Linear fit equations together with the correlation coefficient are given next to corresponding calibration curves. The points on the calibration curve correspond to the signals calculated from the third voltammetric repetition recorded for each concentration.

curve. It is expressed as an absolute value having a unit of A•M^{-1}. Diffusion coefficients were calculated from the positive and negative peak current values (giving information about the analyte diffusivity in the aqueous and the organic phase, respectively) plotted in function of the increasing scan rate (5; 10; 15; 20; 25 and 30 mV•s^{-1}) for the fixed cocaine cutting agent concentration. Rearranged Randles – Ševčík equation was used in this respect: [53]

$$I_p = 2.69 \cdot 10^5 \cdot n^{\frac{3}{2}} \cdot A \cdot D^{\frac{1}{2}} \cdot c \cdot v^{\frac{1}{2}} \quad (4)$$

where D (cm^2•s^{-1}) is the desired value of diffusion coefficient, I_p (A) is the peak current, n is the value of the charge transferred through a polarized LLI during a single event, A (cm^2) is the ITIES area, c (mol•cm^{-3}) is the concentration of the target analyte, and v (V•s^{-1}) is the scan rate.

Also, from the ITVs, we have extracted the values of formal Galvani potentials differences ($\Delta^{aq}_{org}\Phi'$) of the ion (protonated cutting agents) transfer reaction. This parameter provides information about the potential that needs to be applied to the LLI to transfer a molecule from the aqueous to the organic phase. Using $\Delta^{aq}_{org}\Phi'$ and Eq. (5) we have calculated formal Gibbs free energy ($\Delta^{aq}_{org}G'$) of the ion transfer reaction.

$$\Delta^{aq}_{org}G' = -z \cdot F \cdot \Delta^{aq}_{org}\Phi\odot \quad (5)$$

where z and F is the charge and the Faraday constant, respectively. Based on the $\Delta^{aq}_{org}\Phi'$ we also calculated the water||1,2-dichloroethane partition coefficients (the ratio between the concentration of the ion in the organic and aqueous phases, $\log P'_{aq/org}$) using the formula derived from the Nernst-like equation for the ion simple ion transfer reaction [54]:

$$\log \boldsymbol{P'_{aq/org}} = -\frac{\boldsymbol{z} \cdot \boldsymbol{F} \cdot \boldsymbol{\Delta^{aq}_{org}\Phi'}}{2.303 \cdot \boldsymbol{R} \cdot \boldsymbol{T}} = \boldsymbol{log}\frac{\boldsymbol{a_i^{org}}}{\boldsymbol{a_i^{aq}}} \quad (6)$$

where R (8.3145 $\frac{J}{mol \cdot K}$) is the gas constant and T is the temperature (288.15 K), a_i is the activity of the ion (i) in the organic (org) or the aqueous (aq) phase. Electroanalytical and physicochemical parameters for all interfacially active cocaine cutting agents are summarized in Table 2.

K_D is defined as the ratio between the neutral form of the compound in the aqueous and organic phases. Its relationship with these studies will be explained at a later stage in the discussion of the results.

As shown in Table 2, most cocaine cutting agents being active at the ITIES possess the expected magnitude of the LOD and LOQ values equal to a few µM. The exception was caffeine, which signal was significantly overlaid with the potential window limiting current (influencing data treatment) and hydroxyzine for which the calculated LOD was equal to around 25 and 30 µM for positive and negative signal, respectively. The voltammetric sensitivity for studied drugs found in the range from 0.07 to 0.20 A•M^{-1} (values for caffeine and levamisole, respectively) is in line with the 0.06 A•M^{-1} obtained for cocaine [39]. Diffusion coefficients calculated from the scan rate dependencies hold expected order of magnitude and follow the logical order with the 1.3•10^{-6} cm^2•s^{-1} for hydroxyzine (molecule having largest hydrodynamic radius) to 11.1 • 10^{-6}

$cm^2 \bullet s^{-1}$ for diltiazem being significantly smaller. Another important parameter is $logP_{DCE}$ defining studied molecules hydrophobicity. The obtained data show that caffeine and phenylethylamine will be the most hydrophilic, whereas diltiazem is the most hydrophobic cutting agent among all studied species. The difference in the partitioning of the interfacially active drugs is a key aspect defining the system selectivity. Cutting agents with $logP_{DCE} << logP_{DCE(cocaine)}$ should not interfere during cocaine sensing at ITIES.

Fig. 2 shows concentration fraction diagrams plotted for all cocaine cutting agents active at the employed polarized LLI. These plots were prepared using the pK_a values summarized in Table 2. The information provided by the concentration fraction diagram can be directly translated into a pH dependent studied cutting agent species composition in the aqueous phase, in our case BRB. Additionally, on each graph we have marked the pK_a (8.7) [63] value for the cocaine – see green dashed line vertical to the *x*-axis – to indicate the conditions at which the ratio between the protonated and neutral form of cocaine is equal to 1. Careful inspection of all concentration fraction diagrams can be used to optimize the conditions for cocaine sensors development. The pKa values for procaine (Fig. 2A) and diphenhydramine (Fig. 2H) are very close to the pKa value of cocaine meaning that these two molecules will exhibit very similar concentration fraction profiles in the entire pH range. The cocaine detection in the presence of lidocaine (Fig. 2B) and diltiazem (Fig. 2G) should be performed at the pH equal to the cocaine pKa. At these experimental conditions, the fraction of the protonated lidocaine and diltiazem approaches zero, and hence, we expect to observe the largest separation between recorded ionic currents peaks within the voltammetric potential window. The amines above their pKa, although deprived of the charge, can partition to the organic phase and act as the ionophore facilitating the transfer of a proton from the aqueous phase to the organic phase (positive currents) [32,64,65]. The facilitated transfer of proton occurs at potentials higher than the potential of the fully protonated and corresponding amine transfer assuring a positive shift in the voltammetric peak position. The pK_a of levamisole (Fig. 2C), caffeine (Fig. 2E), and phenylethylamine (Fig. 2F) are higher than the pK_a of cocaine meaning that the concentration fraction of the protonated forms of these cutting agents will be always higher as compared with the cocaine close to its pK_a value. Nevertheless, these three molecules (especially caffeine and phenylethylamine) are significantly more hydrophilic and give signals at higher than cocaine Galvani potential difference values (see Fig. 3). The last interfacially active cocaine cutting agent is hydroxyzine having two protonable nitrogen atoms within its heterocycle. Its concentration fraction diagram is shown in Fig. 2D. Dicationic hydroxyzine exists at significant concentrations at pH < 2. This means, that for the conditions applied in this study (pH range from 2 till 11) the aqueous phase mainly contained monocationic (in pH range from 2 to 7) and neutral (pH > 8) hydroxyzine species. Similar to lidocaine and diltiazem, cocaine detection in the presence of hydroxyzine should be performed at pH close to cocaine pK_a as these conditions should assure the largest peak separation.

Using the data obtained from the cyclic voltammograms recorded at different pH values (as the example see Fig. S17 being a series of voltammograms recorded for phenylethylamine) we have plotted the ion partition diagrams where the half-wave Galvani potential difference ($\boldsymbol{\Delta^{aq}_{org}\Phi_{1/2}}$) for the concerned cutting agent is plotted against the aqueous phase pH (see Fig. 3). The aqueous phase pH affects the concentration fraction of the interfacially active species and consequently their interfacial behavior. The change in $\boldsymbol{\Delta^{aq}_{org}\Phi_{1/2}}$ for each of the tested cutting agents was followed experimentally and can be predicted with the eq. 7 [66–68]:

$$\Delta^{aq}_{org}\Phi_{1/2} = \Delta^{aq}_{org}\Phi' + \frac{R \cdot T}{F} \ln\left(\frac{10^{-pH} + K_a + K_a K_D}{10^{-pH}}\right) \quad (7)$$

where $\Delta^{aq}_{org}\Phi\odot$' is the formal Galvani potential difference of the ion transfer reaction; *F* is the Faraday constant, pH has its usual meaning, K_a is the acid dissociation constant calculated from the pK_a value (see Table 2 for numerical values, for hydroxyzine the pK_a was based on its pKa_2 value); and K_D is the distribution constant of the neutral form of cocaine cutting agents between the aqueous and the organic phase as expressed with the eq. 8:

$$\boldsymbol{K_D} = \frac{\boldsymbol{c_C^{aq}}}{\boldsymbol{c_C^{org}}} \quad (8)$$

$\boldsymbol{c_C^{aq}}$ and $\boldsymbol{c_C^{org}}$ stand for concentrations of the studied chemical species with the zero net charge in the aqueous and the organic phase, respectively. K_D was the adjustable variable in the Eq. (7), which appropriate adjustment allows the best fit to the experimental data marked with the solid red line (see Fig. 3). K_D values found for each investigated cocaine cutting agent are listed in Table 2. Due to the difficulty in extracting $\boldsymbol{\Delta^{aq}_{org}\Phi_{1/2}}$ for caffeine and plotting its ion partition diagram the K_D for this molecule is not available.

Fig. 3 summarizes the ion partition diagrams for all cutting agents giving a clear signal within the available voltammetric potential window. This data not only allow careful examination of mechanisms governing pH-dependent interfacial charge transfer reaction but also gives a number of parameters describing molecular partitioning between the aqueous phase and 1,2-dichloroethane. Fig. 3A is a schematic representation of the ion partition diagram (plotted for $pK_a = 9$; $K_D = 1000$) aiming at describing the pH-dependent interfacial charge transfer mechanism common to all cocaine illicit drugs studied in this work. In the pH range for which the concentration fraction of the fully protonated (positively charged, pH << pK_a) studied drug is equal to unity (100%) the recorded ionic currents are due to the simple cation interfacial transfer reaction giving a positive current during the transfer from the water phase to the organic phase and the negative current on its back transfer. At the pH equal to around 5 (value marked with the red solid line perpendicular to the x-axis) the concentration of the monocationic form of the drug in the aqueous phase ($[\boldsymbol{Drug^+_{aq}}]$) is equal to the concentration of the neutral form of the corresponding drug in the organic phase ($[\boldsymbol{Drug_{org}}]$) [39]. From this point, further decrease in the proton concentration results in the positive shift of the $\boldsymbol{\Delta^{aq}_{org}\Phi_{1/2}}$. At pH > pK_a the concentration fraction of the neutral drug species having the ability to spontaneously partition to the organic phase increases. As such, the charge transfer mechanism is switched from the simple ion transfer reaction (protonated drug going from one phase to another) to the facilitated proton transfer reaction (see Fig. 3A for the scheme). Existence of basic amine groups in the organic phase facilities the transfer of a proton from the aqueous to the organic phase giving positive ionic current recorded at voltammetric curves. The shape of the ionic partition diagram is highly related to the neutral form of the drug hydrophilicity/hydrophobicity defined by the distribution constant (K_D see Eq. (8)). The molecules having a higher affinity to the organic phase will have higher values of the K_D factor. The data extracted from Fig. 3B–3G provided the K_D equal to 15,000, 1500, 520, 190, 130, 6.5, and 0.1 for diphenhydramine, levamisole, lidocaine, diltiazem, hydroxyzine, procaine, and phenylethylamine, respectively. The output of this experiment is not surprising since even the inspection of the chemical structures suggests that diphenhydramine should be the most hydrophobic among all interfacially active cutting agents. All parameters related to molecular partitioning are summarized in

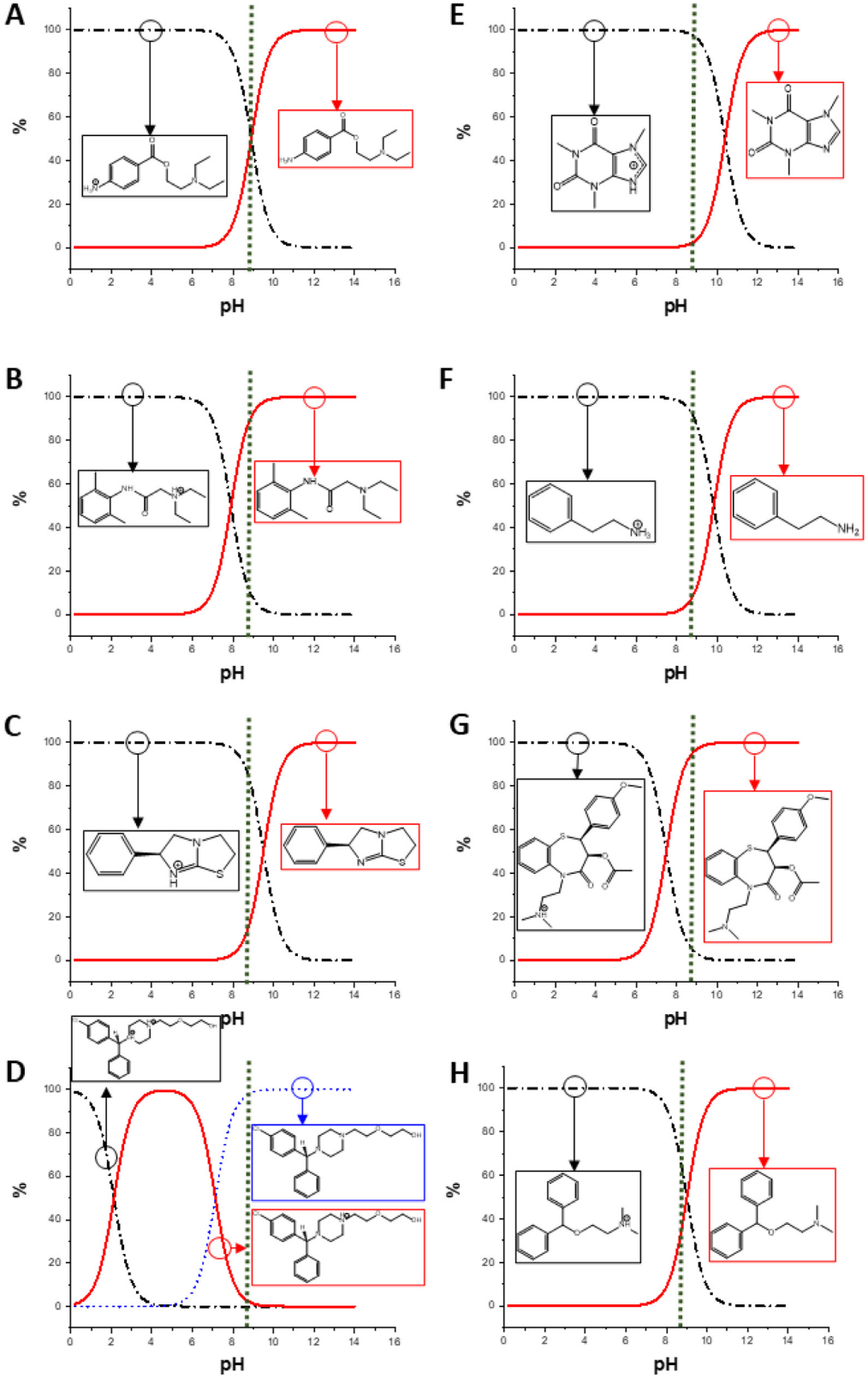

Fig. 2. Concentration fraction diagrams for the cocaine cutting agents being electrochemically active at the electrified LLI. A – procaine, B – lidocaine, C – levamisole, D – hydroxyzine, E – caffeine, F – phenylethylamine, G – diltiazem, H – diphenhydramine. For the pK_a values refer to Table 2. Green dashed line vertical to the *x*-axis indicate the pK_a value for the cocaine.

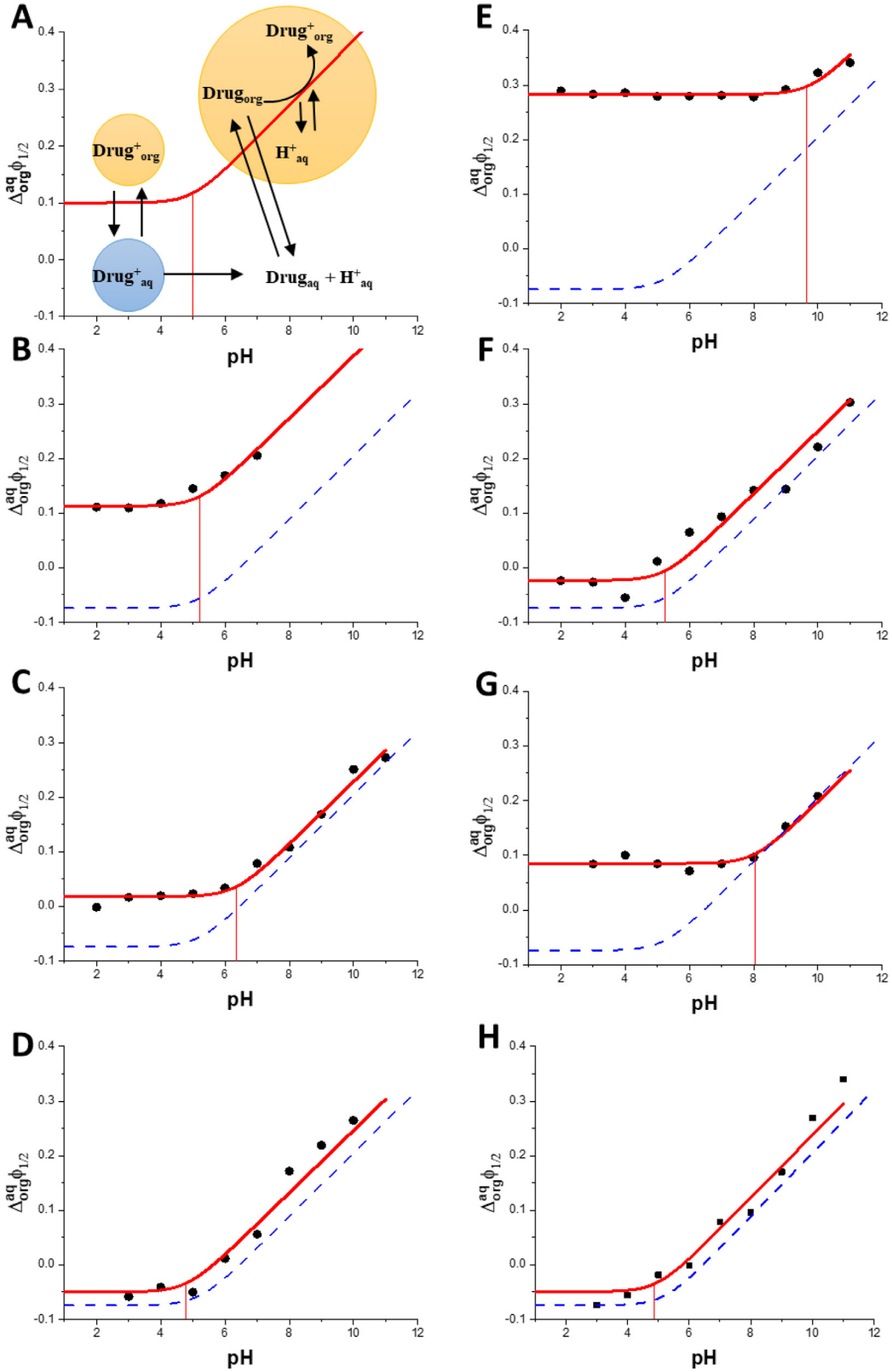

Fig. 3. Ion partition diagrams for the illicit drugs cutting agents being electrochemically active at the electrified LLI (experimental data – black circles, best fit using Eq. (7) – solid red line, theoretical ion partition diagram for the cocaine – dashed blue line). A – an exemplary theoretical diagram with a schematic transfer of ions in individual pH values, B – lidocaine, C – levamisole, D - diphenhydramine, E – phenethylamine, F – diltiazem, G – procaine, H - hydroxyzine. The vertical red line perpendicular to the *x*-axis indicates the pH for which $[Drug^{+}_{aq}] = [Drug_{org}]$ (for details refer to the text).

Table 2. Each subsection of Fig. 3 contains the ion partition diagram for the studied cutting agent (red line) and cocaine (dashed blue line). From the sensing point of view, the signals originating from cocaine, lidocaine (Fig. 3B), and phenethylamine (Fig. 3E) will be sufficiently separated ensuring ITIES based sensor selectivity in the entire pH range. Detection of cocaine in the presence of procaine (Fig. 3G) and levamisole (Fig. 3C) should be performed only at the pH < pK_a of the corresponding cutting agents (in practice pH = 7, see Fig. 2C and G). Caffeine should not constituent a problem since its transfer overlays with the background current on the positive side of the potential window. Cocaine displays interfacial characteristics similar to diphenhydramine (Fig. 3D), diltiazem (Fig. 3F), and hydroxyzine (Fig. 3H), and hence, these three cutting agents are potentially problematic in a view of cocaine detection at ITIES. In the future, we plan to validate the findings presented in this work with other voltammetric methods allowing for better signal deconvolution (AC Voltammetry and differential pulse voltammetry).

4. Conclusions

In this work, the electrified liquid-liquid interface also known as the interface between two immiscible electrolyte solutions was used to study cocaine cutting agents (chemical frequently used to adulterate cocaine street samples). Among 23 chosen target analytes only 8 (procaine, lidocaine, levamisole, hydroxyzine, caffeine, phenylethylamine, diltiazem, and diphenhydramine) were found to give a signal within the available potential window. Based on our results we have provided a number of electroanalytical (voltammetric detection sensitivity, LODs, LOQs), physicochemical (diffusion coefficients, formal Galvani potential difference of ion transfer, formal Gibbs free energy of ion transfer), and pharmacological (partition coefficient, distribution constant) parameters for the interfacially active cutting agents. Based on the obtained results we provided a number of guidelines for the development of a sensor allowing for the selective detection of cocaine in street samples.

Declaration of Competing Interest

The authors declare no conflict of interests

Credit authorship contribution statement

Paulina Borgul: Validation, Formal analysis, Investigation, Data curation, Writing – original draft, Visualization. **Karolina Sobczak:** Formal analysis, Investigation, Writing – original draft. **Konrad Rudnicki:** Validation, Writing – review & editing. **Piotr Glazer:** Validation, Writing – review & editing. **Patrycja Pawlak:** Investigation. **Anna Trynda:** Resources, Writing – review & editing. **Sławomira Skrzypek:** Supervision, Writing – review & editing. **Lukasz Poltorak:** Conceptualization, Methodology, Validation, Writing – original draft, Writing – review & editing, Visualization, Supervision, Funding acquisition.

Acknowledgments

This project was financially supported by the National Science Center (NCN) in Krakow, Poland (Grant no. UMO-2018/31/D/ST4/03259).

Supplementary materials

Supplementary material associated with this article can be found, in the online version, at doi:10.1016/j.electacta.2021.139553.

References

[1] U.N. Publication, World Drug Report 2020, 2020. https://doi.org/10.18356/6ebecec0-en.
[2] B. Yüksel, N. Şen, Development and validation of a gc-fid method for determination of cocaine in illicit drug samples, Marmara Pharm. J. 22 (2018) 511–518, doi:10.12991/jrp.2018.92.
[3] T. Mieczkowski, A research note: the outcome of GC/MS/MS confirmation of hair assays on 93 cannabinoid (+) cases, Forensic Sci. Int. 70 (1995) 83–91, doi:10.1016/0379-0738(94)01628-I.
[4] H.J. Helmlin, K. Bracher, D. Bourquin, D. Vonlanthen, R. Brenneisen, J. Styk, Analysis of 3,4-methylenedioxymethamphetamine (MDMA) and its metabolites in plasma and urine by HPLC-DAD and GC–MS, J. Anal. Toxicol. 20 (1996) 432–440, doi:10.1093/jat/20.6.432.
[5] M. Sergi, E. Bafile, D. Compagnone, R. Curini, G. D'ascenzo, F.S. Romolo, Multiclass analysis of illicit drugs in plasma and oral fluids by LC-MS/MS, Anal. Bioanal. Chem. 393 (2009) 709–718, doi:10.1007/s00216-008-2456-3.
[6] N.V.S. Rodrigues, E.M. Cardoso, M.V.O. Andrade, C.L. Donnici, M.M. Sena, Analysis of seized cocaine samples by using chemometric methods and FTIR spectroscopy, J. Braz. Chem. Soc. 24 (2013) 507–517, doi:10.1590/s0103-50532013000300019.
[7] C.A.F. De Oliveira Penido, M.T.T. Pacheco, I.K. Lednev, L. Silveira, Raman spectroscopy in forensic analysis: identification of cocaine and other illegal drugs of abuse, J. Raman Spectrosc. 47 (2016) 28–38, doi:10.1002/jrs.4864.
[8] J. Eliaerts, N. Meert, F. Van Durme, P. Dardenne, S. Charles, K. De Wael, N. Samyn, Challenges for cocaine detection in smuggling samples, Forensic Sci. Int. 319 (2021) 110534, doi:10.1016/j.forsciint.2020.110534.
[9] M. Klimuntowski, M.M. Alam, G. Singh, M.M.R. Howlader, Electrochemical sensing of cannabinoids in biofluids: a noninvasive tool for drug detection, ACS Sens. 5 (2020) 620–636, doi:10.1021/acssensors.9b02390.
[10] J.M. Freitas, D.L.O. Ramos, R.M.F. Sousa, T.R.L.C. Paixão, M.H.P. Santana, R. a. a. Muñoz, E.M. Richter, A portable electrochemical method for cocaine quantification and rapid screening of common adulterants in seized samples, Sens. Actuators B Chem. 243 (2017) 557–565, doi:10.1016/j.snb.2016.12.024.
[11] K.R. Teófilo, L.C. Arantes, P.A. Marinho, A.A. Macedo, D.M. Pimentel, D.P. Rocha, A.C. de Oliveira, E.M. Richter, R.A.A. Munoz, W.T.P. dos Santos, Electrochemical detection of 3,4-methylenedioxymethamphetamine (ecstasy) using a boron-doped diamond electrode with differential pulse voltammetry: simple and fast screening method for application in forensic analysis, Microchem. J. 157 (2020) 105088, doi:10.1016/j.microc.2020.105088.
[12] A. Florea, M. de Jong, K. De Wael, Electrochemical strategies for the detection of forensic drugs, Curr. Opin. Electrochem. (2018) 1–7, doi:10.1016/j.coelec.2018.06.014.
[13] M. De Jong, A. Florea, A.M. De Vries, A.L.N. Van Nuijs, A. Covaci, F. Van Durme, J.C. Martins, N. Samyn, K. De Wael, Levamisole: a common adulterant in cocaine street samples hindering electrochemical detection of cocaine, Anal. Chem. 90 (2018) 5290–5297, doi:10.1021/acs.analchem.8b00204.
[14] EU Drug Markets Report 2019, Drug production in the EU: monitoring, (drug) law enforcement activities and futures 07, 7AD.
[15] O. Kudlacek, T. Hofmaier, A. Luf, F.P. Mayer, T. Stockner, C. Nagy, M. Holy, M. Freissmuth, R. Schmid, H.H. Sitte, Cocaine adulteration, J. Chem. Neuroanat. 83–84 (2017) 75–81, doi:10.1016/j.jchemneu.2017.06.001.
[16] J. Goldsworth, European Drug Report; Trends and developments, 2020. https://doi.org/10.1093/tandt/ttm111.
[17] A. Trynda, A. Duszyńska, Current trends in purity, quantity and prices of the most popular drugs in Poland, Issues Forensic Sci. 306 (2019) 48–58, doi:10.34836/pk.2019.306.2.
[18] F. Tosato, T.R. Rosa, C.L.M. Morais, A.O. Maldaner, R.S. Ortiz, P.R. Filgueiras, K.M. Gomes Lima, W. Romão, Direct quantitative analysis of cocaine by thin layer chromatography plus a mobile phone and multivariate calibration: a cost-effective and rapid method, Anal. Methods 8 (2016) 7632–7637, doi:10.1039/c6ay02126c.
[19] A. Florea, T. Cowen, S. Piletsky, K. De Wael, Polymer platforms for selective detection of cocaine in street samples adulterated with levamisole, Talanta 186 (2018) 362–367, doi:10.1016/j.talanta.2018.04.061.
[20] R. Zhang, K. Fu, F. Zou, H. Bai, G. Zhang, F. Liang, Q. Liu, Highly sensitive electrochemical sensor based on Pt nanoparticles/carbon nanohorns for simultaneous determination of morphine and MDMA in biological samples, Electrochim. Acta 370 (2021) 137803, doi:10.1016/j.electacta.2021.137803.
[21] M. Parrilla, N.F. Montiel, F. Van Durme, K. De Wael, Derivatization of amphetamine to allow its electrochemical detection in illicit drug seizures, Sens. Actuators B Chem. 337 (2021) 129819, doi:10.1016/j.snb.2021.129819.
[22] R.S. Deinhammer, M. Ho, J.W. Anderegg, M.D. Porter, Electrochemical oxidation of amine-containing compounds: a route to the surface modification of glassy carbon electrodes, Langmuir 10 (1994) 1306–1313.
[23] É.N. Oiye, N.B. De Figueiredo, J.F. De Andrade, H.M. Tristão, M.F. De Oliveira, Voltammetric determination of cocaine in confiscated samples using a cobalt hexacyanoferrate film-modified electrode, Forensic Sci. Int. 192 (2009) 94–97, doi:10.1016/j.forsciint.2009.08.004.
[24] M. De Jong, A. Florea, J. Eliaerts, F. Van Durme, N. Samyn, K. De Wael, Tackling poor specificity of cocaine color tests by electrochemical strategies, Anal. Chem. 90 (2018) 6811–6819, doi:10.1021/acs.analchem.8b00876.
[25] Z. Samec, Dynamic electrochemistry at the interface between two immiscible electrolytes, Electochim. Acta 84 (2012) 21–28, doi:10.1016/j.electacta.2012.03.118.

[26] S. Liu, Q. Li, Y. Shao, Electrochemistry at micro- and nanoscopic liquid/liquid interfaces, Chem. Soc. Rev. 40 (2011) 2236–2253, doi:10.1039/c0cs00168f.
[27] M. de Puit, L. Poltorak, E.J.R. Sudholter, Electrochemical cocaine (bio)sensing. From solid electrodes to soft junctions, TrAC Trends Anal. Chem. 114 (2019) 48–55, doi:10.1016/j.trac.2019.02.025.
[28] S. Zannah, D.W.M. Arrigan, Electrochemistry of catalase at a liquid|liquid micro-interface array, Bioelectrochemistry 138 (2021) 107694, doi:10.1016/j.bioelechem.2020.107694.
[29] M.N. Jajuli, M.H. Hussin, B. Saad, A.A. Rahim, M. Hébrant, G. Herzog, Electrochemically modulated liquid-liquid extraction for sample enrichment, Anal. Chem. 91 (2019) 7466–7473, doi:10.1021/acs.analchem.9b01674.
[30] M.L. Colombo, J.V. Sweedler, M. Shen, Nanopipet-based liquid-liquid interface probes for the electrochemical detection of acetylcholine, tryptamine, and serotonin via ionic transfer, Anal. Chem. 87 (2015) 5095–5100, doi:10.1021/ac504151e.
[31] H.A. Santos, V. García-Morales, C.M. Pereira, Electrochemical properties of phospholipid monolayers at liquid-liquid interfaces, ChemPhysChem 11 (2010) 28–41, doi:10.1002/cphc.200900609.
[32] K. Rudnicki, L. Poltorak, S. Skrzypek, E.J.R. Sudhölter, Ion transfer voltammetry for analytical screening of fluoroquinolone antibiotics at the water –1.2-dichloroethane interface, Anal. Chim. Acta 1085 (2019) 75–84, doi:10.1016/j.aca.2019.07.065.
[33] Š. Skalová, J. Langmaier, J. Barek, V. Vyskočil, T. Navrátil, Doxorubicin determination using two novel voltammetric approaches: a comparative study, Electrochim. Acta 330 (2020) 1–8, doi:10.1016/j.electacta.2019.135180.
[34] F. Kivlehan, Y.H. Lanyon, D.W.M. Arrigan, Electrochemical study of insulin at the polarized liquid-liquid interface, Langmuir 24 (2008) 9876–9882, doi:10.1021/la800842f.
[35] E. Alvarez de Eulate, L. Serls, D.W.M. Arrigan, Detection of haemoglobin using an adsorption approach at a liquid-liquid microinterface array, Anal. Bioanal. Chem. 405 (2013) 3801–3806, doi:10.1007/s00216-012-6622-2.
[36] H. Nagatani, M. Fujisawa, H. Imura, Mechanistic analysis of ion association between dendrigraft poly- l -lysine and 8-anilino-1-naphthalenesulfonate at liquid|liquid interfaces, Langmuir 34 (2018) 3237–3243, doi:10.1021/acs.langmuir.8b00131.
[37] H. Tatsumi, T. Ueda, Ion transfer voltammetry of tryptamine, serotonin, and tryptophan at the nitrobenzene/water interface, J. Electroanal. Chem. 655 (2011) 180–183, doi:10.1016/j.jelechem.2011.02.011.
[38] R. Akter, D.W.M. Arrigan, Detection of prostate specific membrane antigen at picomolar levels using biocatalysis coupled to assisted ion transfer voltammetry at a liquid-organogel microinterface array, Anal. Chem. 88 (2016) 11302–11305, doi:10.1021/acs.analchem.6b03518.
[39] L. Poltorak, I. Eggink, M. Hoitink, E.J.R. Sudholter, M. De Puit, Electrified soft interface as a selective sensor for cocaine detection in street samples, Anal. Chem. 90 (2018) 7428–7433, doi:10.1021/acs.analchem.8b00916.
[40] E. Wang, Z. Yu, N. Li, Anaesthetic lidocaine and dicaine transfer across liquid/liquid interfaces, Electroanalysis 4 (1992) 905–909.
[41] G. Bouchard, A. Pagliara, G.P. Van Balen, P.A. Carrupt, B. Testa, V. Gobry, H.H. Girault, G. Caron, G. Ermondi, R. Fruttero, Ionic partition diagram of the zwitterionic antihistamine cetirizine, Helv. Chim. Acta. 84 (2001) 375–387, doi:10.1002/1522-2675(20010228)84:2⟨375::AID-HLCA375⟩3.0.CO;2-4.
[42] Y. Kubota, H. Katano, M. Senda, Ion-transfer voltammetry of local anesthetics at an organic solvent/water interface and pharmacological activity vs. Ion partition coefficient relationship, Anal. Sci. 17 (2001) 65–70, doi:10.2116/analsci.17.65.
[43] M.L. Colombo, S. McNeil, N. Iwai, A. Chang, M. Shen, Electrochemical detection of dopamine via assisted ion transfer at nanopipet electrode using cyclic voltammetry, J. Electrochem. Soc. 163 (2016) H3072–H3076, doi:10.1149/2.0091604jes.
[44] N.T. Iwai, M. Kramaric, D. Crabbe, Y. Wei, R. Chen, M. Shen, GABA detection with nano-ITIES pipet electrode: a new mechanism, water/DCE–octanoic acid interface, Anal. Chem. 90 (2018) 7b03099 acs.analchem, doi:10.1021/acs.analchem.7b03099.
[45] R. Gulaboski, M.N.D.S.S. Cordeiro, N. Milhazes, J. Garrido, F. Borges, M. Jorge, C.M. Pereira, I. Bogeski, A.H. Morales, B. Naumoski, A.F. Silva, Evaluation of the lipophilic properties of opioids, amphetamine-like drugs, and metabolites through electrochemical studies at the interface between two immiscible solutions, Anal. Biochem. 361 (2007) 236–243, doi:10.1016/j.ab.2006.11.006.
[46] V. Chopineaux-Courtois, F. Reymond, G. Bouchard, P.A. Carrupt, B. Testa, H.H. Girault, Effects of charge and intramolecular structure on the lipophilicity of nitrophenols, J. Am. Chem. Soc. 121 (1999) 1743–1747, doi:10.1021/ja9836139.
[47] Z. Samec, Electrochemistry at the interface between two immiscible electrolyte solutions (IUPAC technical report), Pure Appl. Chem. 76 (2004) 2147–2180.
[48] M.C.A. Marcelo, K.C. Mariotti, M.F. Ferrão, R.S. Ortiz, Profiling cocaine by ATR-FTIR, Forensic Sci. Int. 246 (2015) 65–71, doi:10.1016/j.forsciint.2014.11.011.
[49] R. Dams, T. Benijts, W.E. Lambert, D.L. Massart, A.P. De Leenheer, Heroin impurity profiling: trends throughout a decade of experimenting, Forensic Sci. Int. 123 (2001) 81–88, doi:10.1016/S0379-0738(01)00541-2.
[50] J. Monahan, A.A. Gewirth, R.G. Nuzzo, Indirect fluorescence detection of simple sugars via high-pH electrophoresis in poly(dimethylsiloxane) microfluidic chips, Electrophoresis 23 (2002) 2347–2354 https://doi.org/10.1002/1522-2683(200207)23:14<2347::AID−ELPS2347>3.0.CO;2-G.
[51] S. Beninati, D. Semeraro, M. Mastragostino, Adsorption of paracetamol and acetylsalicylic acid onto commercial activated carbons, Adsorpt. Sci. Technol. 26 (2008) 721–734, doi:10.1260/026361708788251349.
[52] R.T. Kachoosangi, G.G. Wildgoose, R.G. Compton, Using capsaicin modified multiwalled carbon nanotube based electrodes and p-chloranil modified carbon paste electrodes for the determination of amines: application to benzocaine and lidocaine, Electroanalysis 20 (2008) 2495–2500, doi:10.1002/elan.200804385.
[53] T.R.L.C. Paixão, Measuring electrochemical surface area of nanomaterials versus the Randles−Ševčík equation, ChemElectroChem 7 (2020) 3414–3415, doi:10.1002/celc.202000633.
[54] K. Kontturi, L. Murtomäki, Electrochemical determination of partition coefficients of drugs, J. Pharm. Sci. 81 (1992) 970–975.
[55] V. Shoshan-Barmatz, S. Zchut, The interaction of local anesthetics with the ryanodine receptor of the sarcoplasmic reticulum, J. Membr. Biol. 133 (1993) 171–181, doi:10.1007/BF00233797.
[56] A. Karnjanapiboonwong, A.N. Morse, J.D. Maul, T.A. Anderson, Sorption of estrogens, triclosan, and caffeine in a sandy loam and a silt loam soil, J. Soils Sediments 10 (2010) 1300–1307, doi:10.1007/s11368-010-0223-5.
[57] A. Sierra Rebolledo, E.D. Molina, L. Berini Aytés, C.Gay Escoda, Comparative study of the anesthetic efficacy of 4% articaine versus 2% lidocaine in inferior alveolar nerve block during surgical extraction of impacted lower third molars, Med. Oral Patol. Oral Circ. Bucal. 12 (2007) 101–106.
[58] L.S. Zaremba, W.H. Smoleński, Design and application of a levamisole-selective membrane sensor, Ann. Oper. Res. 97 (2000) 131–141, doi:10.1023/A.
[59] S.S. Fortes, T. Barth, N.A.J.C. Furtado, M.T. Pupo, C.M. De Gaitani, A.R.M. De Oliveira, Evaluation of dispersive liquid-liquid microextraction in the stereoselective determination of cetirizine following the fungal biotransformation of hydroxyzine and analysis by capillary electrophoresis, Talanta 116 (2013) 743–752, doi:10.1016/j.talanta.2013.07.062.
[60] P. Carniti, A. Gervasini, S. Biella, Determination of catalyst surface acidity in liquids by a pulse liquid chromatographic technique, Adsorpt. Sci. Technol. 23 (2005) 739–749, doi:10.1260/026361705776316587.
[61] S.P. Lefebvre M, W. Homsy, G. Caille, First-pass metabolism of diltiazem in anesthetized rabbits: role of extrahepatic organs, Pharm. Res. 13 (1996).
[62] E. Topp, M.W. Sumarah, L. Sabourin, The antihistamine diphenhydramine is extremely persistent in agricultural soil, Sci. Total Environ. 439 (2012) 136–140, doi:10.1016/j.scitotenv.2012.09.033.
[63] F. Luan, W. Ma, H. Zhang, X. Zhang, M. Liu, Z. Hu, B. Fan, Prediction of pKa for neutral and basic drugs based on radial basis function neural networks and the heuristic method, Pharm. Res. 22 (2005) 1454–1460, doi:10.1007/s11095-005-6246-8.
[64] S.A. Dassie, Facilitated proton transfer or protonated species transfer reactions across oil|water interfaces, J. Electroanal. Chem. 728 (2014) 51–59, doi:10.1016/j.jelechem.2014.06.020.
[65] F. Reymond, G. Steyaert, P.-A. Carrupt, B. Testa, H.H. Girault, Ionic partition diagrams_ a potential−pH representation.pdf, J. Am. Chem. Soc. 118 (1996) 11951–11957.
[66] L. Poltorak, K. Rudnicki, V. Kolivoška, T. Sebechlebská, P. Krzyczmonik, S. Skrzypek, Electrochemical study of ephedrine at the polarized liquid-liquid interface supported with a 3D printed cell, J. Hazard. Mater. 402 (2021) 123411, doi:10.1016/j.jhazmat.2020.123411.
[67] M. Nakamura, T. Osakai, Evaluation of the membrane permeability of drugs by ion-transfer voltammetry with the oil|water interface, J. Electroanal. Chem. 779 (2016) 55–60, doi:10.1016/j.jelechem.2016.05.005.
[68] T. Osakai, H. Yamada, H. Nagatani, T. Sagara, Potential-dependent adsorption of amphoteric rhodamine dyes at the oil/water interface as studied by potential-modulated fluorescence spectroscopy, J. Phys. Chem. C 111 (2007) 9480–9487, doi:10.1021/jp0723315.